

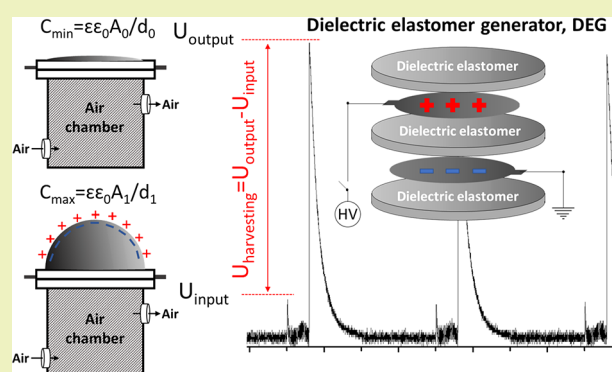
Stretchable Energy Harvesting Devices: Attempts To Produce High-Performance Electrodes

Codrin Tugui,[†] Cristian Ursu,[†] Liviu Sacarescu,[†] Mihai Asandulesa,[†] George Stoian,[‡] Gabriel Ababei,[‡] and Maria Cazacu^{*,†}[†]Inorganic Polymers Department, Petru Poni Institute of Macromolecular Chemistry, Aleea Grigore Ghica Voda 41A, 700487 Iasi, Romania[‡]National Institute of Research and Development for Technical Physics, Str. Professor Dr. doc. Dimitrie Mangeron 47, 700050 Iasi, Romania

S Supporting Information

ABSTRACT: Dielectric elastomer transducers (DETs), essentially consisting of highly deformable insulating films sandwiched between electrodes, are able to convert mechanical work in electrical energy and vice versa. Although still immature, these represent a simple and low-cost alternative to already known technologies for harvesting energy from renewable sources, in this case converting environmental mechanical energies (e.g., wave energy, human body movement) to an electrical one. However, the development of this new technology raises several challenges in terms of finding more efficient materials. For high conversion efficiencies, a dielectric film should meet certain properties such high breakdown strength and small mechanical hysteresis, while the electrodes should be compliant and able to keep conductivity along repeated large deformations. Regarding these aspects, two types of electrodes were successfully achieved, an ultrathin silver electrode of about 40 nm thickness and a PDMS-carbon black composite rubber electrode of about 30 μm thickness. Both electrodes were analyzed in terms of morphology and electrical and mechanical behaviors, as well as actuation response. The results indicate that the rubber electrode is more appropriate because it has proved to work perfectly in hundreds of cycles at large deformations (150%) without losing conductivity. On this basis, three types of capacitors with 120 mm diameters with coaxial electrodes of 60 mm diameters having one (DEG I), two (DEG II), and three (DEG III) active layers were built by a simple and efficient method using a commercial silicone (Elastosil) as the dielectric. The achieved arrays were tested in an energy-harvesting setup. At 200% strain and a bias voltage of 3 V μm^{-1} , DEG I produced 0.07 mJ, DEG II produced 0.2 mJ, and DEG III produced almost 1 mJ with an energy density of 1.1 kJ m^{-3} .

KEYWORDS: Energy harvesting, Sustainable energy, Renewable energy, Dielectric elastomer transducer, Dielectric elastomer



■ INTRODUCTION

In the context of global warming and finite natural resources, new materials hold the key to fundamental advances in free energy conversion. Harvesting energy using dielectric elastomer transducers (DET) represents a great possibility of converting mechanical environmental energies (like oceans waves energy, body motion) directly into electrical energy.^{1–7} Dielectric elastomer transducers are polymeric thin films, usually made of silicones, polyurethanes, or acrylics, coated on both sides with compliant and highly conductive electrodes that allow a large amount of deformation.⁸ Besides operating as generators, they can work as actuators by converting the electrical energy to mechanical work or sensors.^{9–11} Both modes of operation require stretchable and highly conductive electrodes.

From the perspective of development of new generators or actuators based on electroactive polymers, the main factors that influence their performance can be easily identified in the

fundamental equations that describe the required processes, such as DET stretchability, dielectric permittivity, and applied electric field.^{12,13} In this context, numerous studies were oriented on improving the dielectric permittivity of the dielectric through various methods such as the incorporation of various fillers,^{14–16} chemical modification of the elastomer matrix,^{17–19} or interpenetrating different polymers.^{20–24} On the other hand, finding suitable electrodes for DET applications represents a great challenge. Typical electrodes used for dielectric elastomers are usually based on carbon powders or carbon nanotubes, either dispersed in greases or directly deposited on the dielectric surface through various methods as thin layers, but those can suffer from several limitations such as limited pot-life, creep under gravity,

Received: April 30, 2017

Revised: July 13, 2017

Published: July 28, 2017

high resistivity, or mechanical abrasion.^{25–27} The alternatives offered by highly conductive metallic electrodes may exhibit some restrictions related to Young modulus, deformability, or small-scale patterning.^{28–32} However, intensive efforts have been conducted to design electrodes with suitable mechanical properties while keeping a high electrical conductivity over a large number of repeated deformations.^{33–38} Moreover, by using very long silver nanowires able to form percolation networks, highly stretchable and highly conductive electrodes were obtained that can develop large uniaxial strain without being affected by the electrical properties,^{39–46} but the electrodes for DET applications should sustain high biaxial strains.²⁵

In this paper, we focused on obtaining highly compliant electrodes for dielectric elastomers through both a physical and a chemical method. In the first approach, we deposited an ultrathin silver electrode, of about 40 nm, straight on the dielectric film (Elastosil) through the Pulsed Laser Deposition (PLD) technique. The techniques for silver electrodes deposition, mainly used in flexible electronics, consist of solution spray-coating, vacuum filtration followed by transfer, and drop-casting.³⁸ Two procedures for depositing metallic (as implanted nanoclusters) electrodes on silicone are reported in the literature: Filtered Cathodic Vacuum Arc (FCVA) implantation and Supersonic Cluster Beam Implantation (SCBI).²⁵ PLD is one of the simpler, cheaper, and more versatile methods of depositing thin films, for a very wide range of materials, on a wide variety of substrates, at room temperature.⁴⁷ The second strategy was intended to fabricate polydimethylsiloxane (PDMS)–carbon black (PDMS-Cb) composites soft electrodes by incorporating carbon black particles into a silicone matrix. Rubber electrodes based on commercial silicone kits inevitably become more rigid by incorporating carbon black, and this will implicitly lead to increased rigidity of the array. To minimize this effect, the electrode needs to be much thinner than the dielectric. Another measure would be the incorporation of a more efficient conductive filler such as carbon nanotubes or exfoliated graphite having a very high specific surface area and reaching the percolation threshold at low concentrations so as not to induce a significant increase in stiffness.^{25,48}

The originality of our approach is that the rubber electrode with mechanical properties close to those of the dielectric chosen is made. For this purpose, following the preliminary tests, it was found that a customized polydimethylsiloxane with a molecular mass of around $200,000 \text{ g mol}^{-1}$ cross-linked through the ends of the chains is suitable as a matrix because by incorporating 25 wt % carbon black, as needed to achieve good conductivity, the desired mechanical properties are obtained. Moreover, these electrodes have been obtained as free-standing, configurable in any shape and size, easy to handle, and applied on the dielectric. Considering the economic aspects, the carbon black particles represent the cheapest powder from the market that can be used as a conductive filler. The obtained electrodes were investigated from morphological, mechanical, and electrical points of view. For a better evaluation, both types of electrodes were used in a “sandwich” configuration with a common commercial DE in order to evaluate their efficiency in actuation mode. The rubber electrodes in a proper array were tested as conversion units in an energy harvesting setup to assess their suitability regarding the promising energy harvesting technology developed by Fontana and Vertechy.^{2,49–51} The same commercial elastomer as in the case of actuation measurements was used as the active layer.

RESULTS AND DISCUSSION

Regardless of the DET's applications, a conductive and flexible electrode that survives a large number of deformations is required. In this regard and taking into consideration the economic aspects, two types of electrodes were achieved, a highly conductive silver electrode and a highly stretchable free-standing PDMS–carbon black (PDMS-Cb) electrode using a versatile physical method and a straightforward chemical method, respectively (Figure 1).

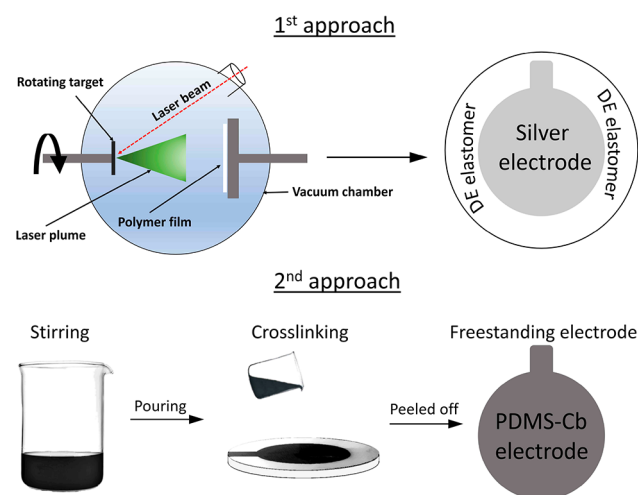
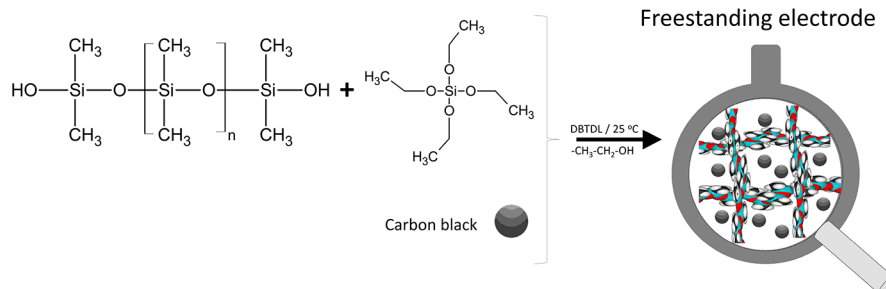


Figure 1. Schematic representation of the path of silver electrodes deposition (top) and for obtaining free-standing electrodes (bottom).

Silver electrodes were deposited at room temperature on both sides of circular commercial films of 100 mm diameter, 25% equiaxial prestrained, through the Pulsed Laser Deposition technique. In order to benefit from a large radial dimension of the laser ablation plume, the polymeric film was placed 15 cm away from the target surface. Moreover, for longer target to substrate distances, lower kinetic energies particles condensation that expand in radial directions with respect to the normal to the target surface are avoided. Thus, the conductive layer will be constituted preponderantly by the high kinetic energy-ablated particles leading to a stronger adhesion of the silver film to the PDMS substrate. A mask was used to protect specific zones that will remain free of electrodes.

In a second approach, a rubber electrode was prepared on the basis of silicone as the dielectric but chosen and engineered in a such way that to be conductive without significantly affecting its elastic properties. This was obtained by incorporating conductive carbon black particles within a high molecular mass polydimethylsiloxane- α,ω -diol (PDMS) ($M_n = 230,000 \text{ g mol}^{-1}$), subsequently cross-linked by condensation with tetraethylorthosilicate in the presence of an organometallic compound (DBTDL) to generate the matrix. Although the molecular weight of the polymer is high, it preferred this cross-linking system through condensation of chain ends resulting in a relatively low cross-link density and thus a soft material. By increasing the amount of carbon black, the rigidity of the electrode increases rapidly thus affecting the mechanical properties. So, after several formulations, the best results were obtained by adding 25 wt % of conductive filler. For a good dispersion of the filler in the matrix, mixing the two was done in the presence of a small addition of solvent (toluene) and composite as solution poured as shaped film on a Teflon

Scheme 1. Cross-linking Reaction Leading to Free-Standing Rubber Electrode



substrate and stabilized by subsequent cross-linking and aging in environmental conditions (Scheme 1, Figure 1, bottom).

Morphological Properties. Both metal and rubber electrodes have a smooth surface without visual defects and a uniform thickness (Figure 2a, d, e). Scanning electron microscopy (SEM)

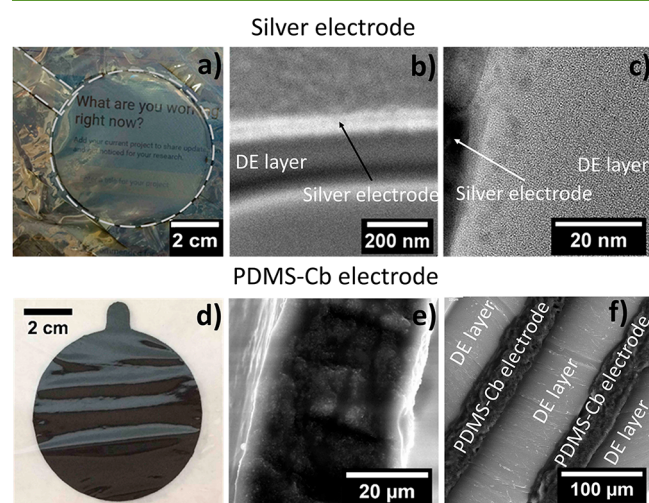


Figure 2. Microscopic images of the two electrodes: (a) top view of silver electrode, (b) FIB-SEM image of dielectric-silver electrode taken in cross-section, (c) FIB-TEM image of silver electrode-silicone film taken at interface, (d) top views of PDMS-Cb electrode, (e) SEM image of PDMS-Cb electrode taken in cryofractured section, and (f) SEM image of PDMS-Cb electrode; DE layer “sandwich” taken in cross-section.

images of the silver electrode show a compact structure having a thickness of about 40 nm (Figure 2b, Figure S1), while the PDMS-Cb electrode images taken on a cryofractured section reveals a uniform distribution of carbon particles within the polymer matrix, the achieved electrode having around 30 μm thickness (Figure 2f). By lowering the PDMS-Cb thickness, the electrodes become very fragile and difficult to handle. Transmission electron microscopy (TEM) image shows that the silver particles penetrate the polymer surface and form small aggregates of few nanometres (Figure 2c). The presence of aggregates is also evidenced by small angle X-ray scattering (SAXS) measurements (Figures S2, S3). Interpretation of the SAXS data was done using the Beaucage unified field theory applied on two-dimensional levels evidenced in the scattering curve (Supporting Information). The unified field modeling results indicate an average dimension of the primary Ag nanoparticles around 6.5 nm. The particles are largely aggregated in clusters with a mass fractality that indicates a high density. The calculated correlation length

suggested that the average distance between the Ag nanoparticles within the aggregates is around 2 nm.

Mechanical Properties. Beside other features, mechanical behavior represents an important aspect regarding the electrode performance in a DET configuration. Young’s modulus calculated at 50% strain shows a slight increase, from 0.54 MPa for pure DE to 0.64 MPa for an array with both sides deposited electrodes. It follows that the metallic layer has an insignificant impact on the dielectric elastomer stiffness. Stress-strain tests also reveal that the silver deposition has a slightly reinforcing effect that leads to an increase in the elongation at break from 420% for pure DE to 500% strain for the achieved “sandwich” (Figure 3). On the other side, the free-standing PDMS-Cb

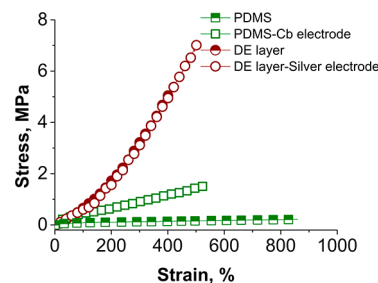


Figure 3. Stress-strain curves for PDMS film, single dielectric (DE) film (Elastosil), and the achieved dielectric-electrodes arrays.

electrode has a Young’s modulus at 50% strain of 0.59 MPa, and an elongation at break of about 530%, as compared with the PDMS film without carbon black that has an elongation at break of 850% and a Young’s modulus at 50% strain of 0.14 MPa (Figure 3).

Electrical Properties. Of course, the main characteristic of an electrode is represented by the electrical conductivity and its ability to keep it until large strains. Thus, both silver and rubber electrodes were tested from this point of view. For their characterization, a standard method, four-point technique, suitable for thin films was used to measure conductivity at different values of strain. As was expected, the electrical conductivity of the silver electrode decreases dramatically with the degree of stretch, from around 1400 S cm^{-1} at 0% strain to 1.6 $\times 10^{-13}$ S cm^{-1} at 300% strain (Figure 4). However, the metallic electrode maintains its conductivity until 10%–20% strain; after that, it is presumed that the formed cracks on the electrode become wider, being able to discontinue the conductivity. Cracks occur due to the stiffness difference between the metallic layer and the soft elastomer. Besides excellent mechanical properties such low Young’s modulus and high stretchability, the prepared free-standing PDMS-Cb electrodes exhibit excellent electrical properties, with the electrical conductivity being unaffected by

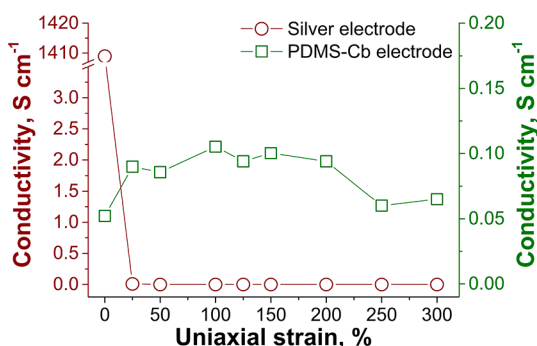


Figure 4. Electrical conductivity of the two electrode types as a function of uniaxial strain.

the uniaxial strain (Figure 4). In this case, the uniaxial strain has a positive effect on the electrode conductivity, increasing from 0.05 S cm^{-1} at 0% strain to 0.06 S cm^{-1} at 300% strain, with the maximum value of about 0.1 S cm^{-1} being in the range of 100%–150%. This phenomenon can be assigned to the reorganization of carbon particles within the polymer matrix, thus achieving the percolation threshold.

Considering that many applications require equibiaxial strains, the PDMS-Cb electrodes were also tested from this perspective. Figure 5 shows that the equiaxial strain slightly decreased the

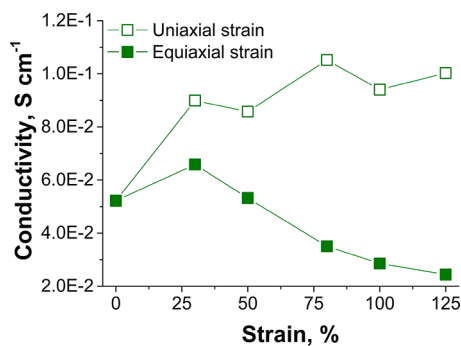


Figure 5. Electrical conductivity of PDMS-Cb electrode vs uniaxial and equiaxial strain.

electrode conductivity from $5 \times 10^{-2} \text{ S cm}^{-1}$ at 0% strain to $2 \times 10^{-2} \text{ S cm}^{-1}$ at 125% strain, while in an uniaxial configuration the conductivity increases with strain, with 125% strain being the upper limit of the setup (Figure S4).

Electromechanical Properties. Actuation Measurements. For a deep evaluation of the electrodes performance from the application perspective, actuation tests were performed on both types of electrodes. The actuation measurements were performed by a stepwise increase in the applied electric field until the breakdown occurred. The results obtained with arrays fabricated using the achieved electrodes and commercial silicone DE are presented in Figure 6. Lateral strain values achieved as a result of an applied electric field show a large difference between arrays with the two electrodes, the maximum lateral strain of PDMS-Cb (22.5% at $75 \text{ V } \mu\text{m}^{-1}$) being several times larger than in the case of using a silver electrode (2.2% at the same voltage). Analyzing the electrical and mechanical information presented above, we can conclude that the PDMS-Cb electrodes being more flexible have the ability to keep the conductivity until a large strain, and the actuation results are logical. Moreover, at higher electric fields, parallel cracks occur on a silver electrode during

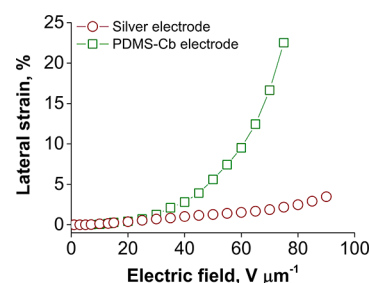


Figure 6. Actuation results of commercial DE assembled with different electrodes.

the actuation strain, which may also limit the displacement (Figure S6).

Energy-Harvesting Measurements. Because the PDMS-Cb electrodes showed the best mechanical, electrical, and actuation results, these were further evaluated as electrodes for dielectric elastomer generators (DEG). To test the electrodes suitability in such applications, these were concentrically attached on the DE layer by slow pressing; the electrode and the dielectric film stay together due to the sticky and common nature of both layers. However, to keep the peripheral electrodes attached on the dielectric, two supplementary elastomer layers were used, and these coatings play as well a safety role. Three DEGs having one (DEG I), two (DEG II), and three (DEG III) active layers, respectively, were built (Figure 7). The active layer of DEG is the DE layer that is electrically charged when a voltage is applied.

The conversion of mechanical energy into electrical energy was performed on a homemade setup adapting the model developed by Fontana and Verthey;² the energy harvested is based on the difference in the DEG capacitance (Figure S7). The dielectric generators were fastened on top of a cylindrical air chamber so they could be inflated. The stretch degree of DEGs can be chosen by varying the inside pressure of the air chamber (Figures S8–S12). As Figure 8 reveals, due to the difference of DEG capacitances and considering the charge, Q is kept constant during DEG relaxation, and the output voltage U_{output} will be bigger than the input voltage U_{input} , the difference $U_{\text{output}} - U_{\text{input}}$ characterizing the energy harvesting concept.⁵²

Figure 9 shows that, depending on the number of DEG active layers, the $U_{\text{output}}/U_{\text{input}}$ ratio increases as the inflating strain increases. In the first case, by applying an input voltage, $U_{\text{input}} = 100 \text{ V}$ on the DEG I, the output voltage increased about 5 times at a 200% strain (Figure 9; Figures S13, S14). In the case of DEG II, by applying the same input voltage $U_{\text{input}} = 100 \text{ V}$, the $U_{\text{output}}/U_{\text{input}}$ ratio increases almost linearly with the inflating strain, with 200% strain U_{output} being around six times bigger than U_{input} (Figure 9; Figures S13, S15). In the third case, the $U_{\text{input}}/U_{\text{input}}$ ratio increases linearly until 100%, then has a sharp increase. Thus, by applying a $U_{\text{input}} = 100 \text{ V}$ on DEG III, at 200% strain, the output voltage U_{output} increases 10 times as compared to the input voltage (Figure 9; Figures S13, S16).

Considering that the dielectric elastomer is incompressible and knowing its characteristics (thickness, area, dielectric permittivity Figure S17), the output energy of the DEG can be calculated (Figure 10). The harvested energy by the stretchable capacitor, W_{harv} was calculated according to eq 1, where W_{out} is the output energy of DEG, W_{in} is the input energy of DEG, C_{max} represents the capacitance of the stretched DEG, C_{min} is the DEG capacitance in flat position, U_{input} is the input voltage, and U_{output} is the measured output voltage.

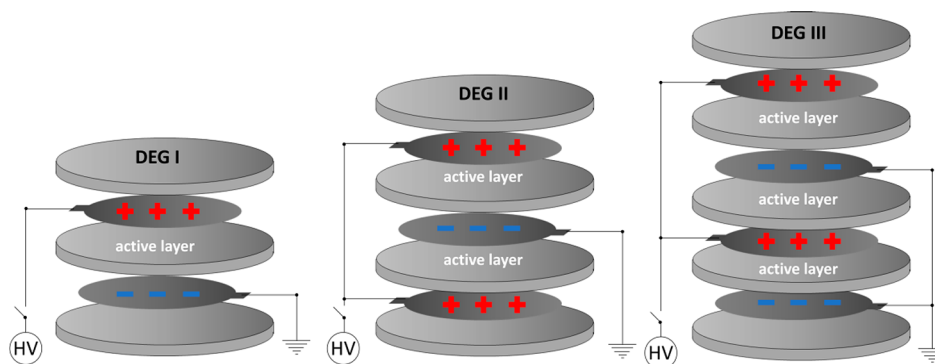


Figure 7. Dielectric elastomer generators (DEGs) having one, two, and three active layers.

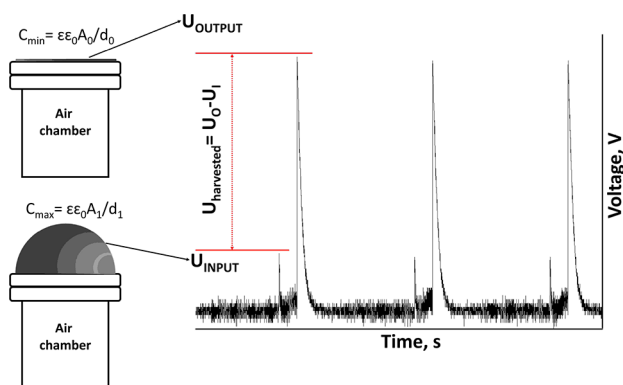


Figure 8. Output voltage vs input voltage during a harvesting cycle.

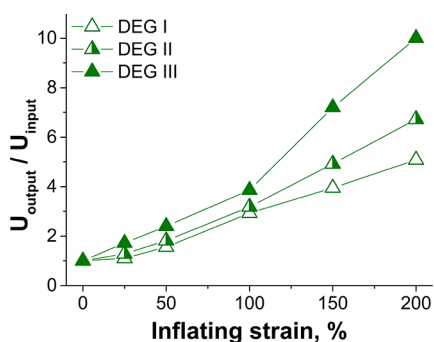


Figure 9. Measured U_{output}/U_{input} ratio as a function of inflating strain, $U_{input} = 100$ V.

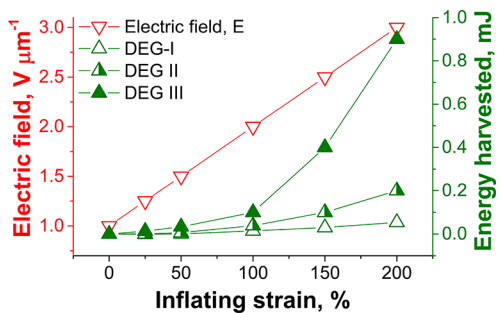


Figure 10. Calculated output energy of DEGs and the electric field as a function of inflating strain at an input voltage of 100 V.

$$W_{harv} = W_{out} - W_{in} = \frac{1}{2}(C_{min}U_{output}^2 - C_{max}U_{input}^2) \quad (1)$$

The applied electric field on the membrane was calculated considering that the DE thickness is changing during inflating. It is observed that this increases linearly with the strain. On the other side, the harvested energy plot has a similar trend as in the case of the U_{output}/U_{input} ratio. The maximum harvested energy was obtained at 200% strain, this being the highest electric field and difference between C_{max} and C_{min} . At 200% strain, DEG I produced 0.07 mJ, DEG II produced 0.2 mJ, and DEG III produced almost 1 mJ.

Normally, the experimental energy density increases as the bias voltage increases (Figure 11). The experimental energy

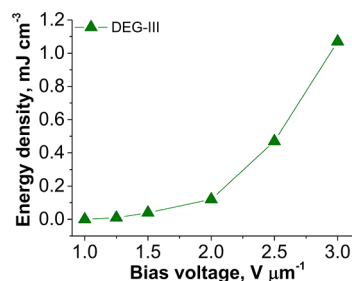


Figure 11. Energy density of DEG III as a function of bias voltage.

density increased from 0.01 mJ cm^{-3} at a bias voltage of $1 \text{ V } \mu\text{m}^{-1}$ to 1.1 mJ cm^{-3} at $3 \text{ V } \mu\text{m}^{-1}$. Similar results were obtained by Yin et al., where by applying a bias voltage of about $4.5 \text{ V } \mu\text{m}^{-1}$ they obtained an energy density of about 1.7 mJ cm^{-3} .⁵³

Moreover, DEG I was subjected to 325 repeated harvesting cycles to evaluate its sustainability. As Figure 12 reveals, after hundreds of cycles, the inside pressure and the output voltage are maintained at the same values (Figure S18).

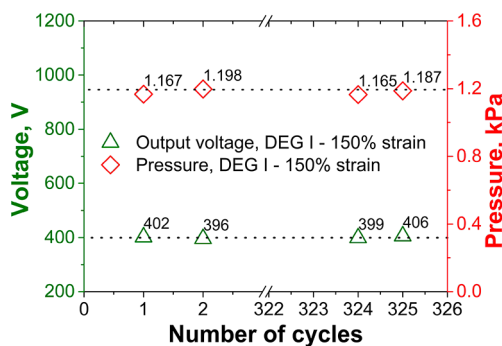


Figure 12. Measured U_{output} and pressure of DEG I dependent on the cycle number.

Thus, ranging the number of dielectric layers and analyzing the obtained results after a few hundreds of harvesting cycles, we found that the fabricated electrodes meet all the requirements for their use in these types of applications. The assembling of the laminated system represents an easy task, and the composite electrode need not be glued on the dielectric layer. Unfortunately, due to the large number of experimental parameters (harvesting configuration, dielectric type, strain, electric field, dielectric permittivity, and so on), the obtained results are difficult to compare with those already reported in the literature.

CONCLUSIONS

Two types of electrodes, one silver (deposited by PLD) and another conductive rubber (based on silicone–carbon black composite), were prepared for the same type of dielectric consisting of a commercial silicone elastomer, Elastosil. While the silver was deposited directly on the dielectric once was generated by laser technique, rubber-like electrodes were independently prepared as free-standing films and subsequently assembled in stacks with the desired number of layers. The results of the TEM and SAXS studies correlate well and reveal that the produced silver particles during the deposition penetrates the polymer surface and generates aggregates of a few nanometers next to the polymer surface. Scanning electron microscopy images of the PDMS-Cb electrode showed a homogeneous structure, with the carbon nanoparticles being well dispersed within the PDMS matrix. The mechanical test results showed that the deposited metallic layer slightly adversely affects the elastomer elasticity, although the elongation at break increases. PDMS-Cb showed also a low Young's modulus, 0.59 MPa, and a high elongation at break of about 500%. The electrical measurements point out that, in the case of the silver electrode, the electrical conductivity decreases drastically with strain, while in the case of rubber electrode the conductivity increases with the strain from 0.005 S cm⁻¹ at 0% strain to 0.1 S cm⁻¹ at 150% strain. Moreover, the electrical conductivity remained almost unchanged until 300% strain and a few hundreds of harvesting cycles at 150% strain. The actuation measurements are consistent with conductivity measurements, and the PDMS-Cb electrode showed much higher displacement before the breakdown occurs, as compared with the silver electrode. Furthermore, by using a simple and efficient method, three “sandwiches” made from PDMS-Cb electrodes and commercial elastomer (Elastosil) were built and tested in an energy harvesting setup. The obtained results showed that the achieved electrodes work perfectly under large strains and after hundreds of repeated harvesting cycles.

EXPERIMENTAL SECTION

Materials. Polydimethylsiloxane- α,ω -diol (PDMS), having $M_n = 230,000$ g mol⁻¹ was synthesized by cationic ring-opening polymerization of octamethylcyclotetrasiloxane in the presence of a cation exchanger as catalyst.⁵⁴ Dibutyltin dilaurate (DBTL) 95%, tetraethylorthosilicate (TEOS), and carbon black (acetylene, 50% compressed, 99.9+% S.A 75 m² g⁻¹ bulk density) were supplied by Alfa Aesar, Germany, and a silver target of 99.95% purity was purchased from Goodfellow and used as such. The Elastosil films having a 100 μ m thickness were purchased from Wacker Chemie, Germany.

Measurements. The stress–strain tests were performed on dumbbell-shaped samples on a TIRA test 2161 apparatus, Maschinenbau GmbH Ravenstein, Germany. The measurements were done in laboratory conditions at an extension rate of 50 mm min⁻¹.

Dielectric properties of the Elastosil film were determined on a Novocontrol Concept 40, GmbH Germany, in a frequency range between 10⁰ and 10⁶ Hz at room temperature.

The cross-section morphology of the PDMS-carbon black electrode was studied by scanning electron microscopy on a ESEM type Quanta 200 equipment in low vacuum mode. The thin electrodes were fractured under liquid nitrogen.

A Cross Beam System Carl Zeiss NEON 40EsB was used with a thermal Schottky field emission emitter, accelerated Ga ions column:electron beam resolution of 1.1–2.5 nm for $U = 20 \div 1$ kV, ion beam resolution of 7 nm at 30 kV, magnification of 12x \div 2,600,000x (SEM) and 635x \div 1,500,000x (FIB). The system is equipped with EDS, EBSD, In-lens and EsB detectors, Gas Injection System (GIS) with five separate nozzles, ion-beam nanopatterning module, and micro-manipulator for TEM samples preparation. The TEM lamella was prepared by the *in situ* lift-out technique. The region of interest is first covered by a protecting material (platinum) by using the GIS in the Crossbeam System. Holes are FIB milled on each side of the lamella, which is then lifted out by a micromanipulator and glued on a support (TEM grid) where the final thinning takes place. An image-corrected Zeiss Libra 200MC transmission electron microscope operated at 200 kV with S-TEM (scanning-TEM) and FFT (fast Fourier transformation) options was used for high resolution microstructural investigations of the sample.

Small angle X-ray scattering (SAXS) measurements were made on a Bruker NanostarU instrument with an X-ray ImS microsource having a copper anode and a three-pinhole collimation system. A Vantec-2000 2D detector with 68 mm resolution was used to record the scattered intensity, $I(q)$. The scattered intensity was measured as a function of the momentum transfer vector $q = 4\pi \sin \theta / \lambda$, where λ is the wavelength of the X-rays (Cu K α radiation, 1.54 Å), and θ is half the scattering angle. The distance from sample to detector was 107 cm, being able to measure q values between 0.008 and 0.3 Å⁻¹. Square pieces of about 6 mm \times 6 mm of silver electrode deposited on Elastosil films were used for this investigation. Before recording, the samples were maintained at 25 °C for 8 h.

The four-point probe technique is a standard method for accurate characterization of the electrical properties (e.g., bulk resistivity) of thin films. The method provides fast, precise, and reproducible measurements since the collected data are not affected by the contact shape and size.⁵⁵ The resistivity four-point probe head operates in collinear mode and encloses four equally spaced pins in contact with the material under test. Accordingly, with the measurement procedure, a direct current is applied through the outer probes, and the corresponding voltage drop over the inner probes is recorded. The configuration includes an Electrometer/High Resistance Meter (Keithley Model 6517A). Considering that the pins are equally distanced and the sample thickness, s , is much smaller than the interprobe spacing, the bulk resistivity is expressed by

$$\rho = \frac{\pi s U}{\ln 2 I} \quad (2)$$

where U is the measured voltage drop, and I is the constant current applied through the outer probes. The electrical conductivity will be further determined by inverting the sample resistivity, $\sigma = 1/\rho$.

Energy harvesting measurements were performed on circular silicone films of 120 mm diameter having coaxial circular electrodes of 60 mm diameter on both sides. The free-standing “sandwiches” were fastened by a ring with the inner diameter of 70 mm at the end of a vertical cylinder; thus, the membrane can be inflated by applying a pneumatic pressure inside the cylinder. The inflating level of the membrane was measured with a laser device (Keyence IL-100), and the inside pressure was monitored with a pressure sensor (MPX12). A high-voltage Trek 20/20C-Hs amplifier connected to an AFG 3000 wave generator were used to supply the voltage. A energy harvesting cycle includes four stages: (1) The uncharged dielectric elastomer generator (DEG) is pneumatically inflated using a commercial compressor up to a certain value. (2) When the system reaches the desired stretch, the DEG is instantaneously charged U_{input} . (3) The compressed air is released from the air chamber; thus, the DEG returns to its original shape keeping the

charge constant. (4) When the system reaches its original configuration and has the minimum capacitance, the DEG is discharged to the ground, U_{output} . To synchronize all steps, we used three relays (a HM12-1A69-150 and two commercial ones) that are controlled via ArbExpress software. The difference between the input voltage (U_{input}) and output voltage (U_{output}) practically characterizes the energy harvesting concept; thus, the electrical energy harvested over a cycle was indirectly determined by measuring the input/output voltage via an HV probe (Tektronix P6015A) connected to a digital oscilloscope (LeCroy WaveAce 2034). Due to safety reasons, the input voltage V_{input} did not exceed 100 V.

The actuation measurements were performed according to ref 24 on circular samples. The PDMS-carbon black electrode of 8 mm diameter was concentrically attached by pressing on both sides of the elastomer. The lateral displacement was optically measured using a digital camera (Figure S5).

Procedure. Preparation of Silver Electrode by Pulse Laser Deposition (PLD). The silver metal deposition was performed on Elastosil film using a circular shaped mask with a diameter of 8 mm for actuation measurement and 60 mm for electrical measurements. All depositions were performed in a vacuum chamber evacuated at 10^{-5} Pa to avoid sample contamination from residual gas. The KrF excimer laser beam (248 nm wavelength, 20 ns the pulse length) was directed at 45° incidence angle on the silver target. The laser fluence was set to 3 J cm^{-2} , and the total number of pulses used for ablation was 40,000 delivered at 20 Hz.

Preparation of Rubber Electrode. In the first stage, 2 g of polydimethylsiloxane- α,ω -diol (PDMS) with a molecular mass $M_n = 230,000 \text{ g mol}^{-1}$ was dissolved in 80 mL of toluene and magnetically stirred in laboratory conditions for 24 h until the polymer was completely dissolved, afterward 0.5 g of carbon black was slowly added. During stirring, the obtained solution was sonicated five times for 5 min. Further, in a Berzelius glass of 10 mL, 7 mL of composite solution, 0.05 mL of tetraethyl orthosilicate (TEOS), and around 0.01 mL of dibutyltin dilaurate (DBTDL) were stirred vigorously and sonicated for 1 min again and quickly poured into a circular frame and left for 24 h in environmental conditions to allow cross-linking and to evaporate the solvent and the condensation byproducts. The formed films were carefully peeled off from the substrate and were left in normal conditions for 2 weeks to allow complete curing.

■ ASSOCIATED CONTENT

Supporting Information

The Supporting Information is available free of charge on the ACS Publications website at DOI: 10.1021/acssuschemeng.7b01354.

FIB-SEM and SAXS data related to silver electrode; images of device for film stretching setup; silver electrode deposition procedure and actuated silver electrode; scheme for energy harvesting setup; graphics of pressure dependence on number of dielectrics; measured output voltage and inflating pressure as a function of inflating strain; harvested voltage of DEG with one, two, and three dielectric layers; dielectric spectrum for dielectric elastomers; and variation of harvested voltage and air chamber pressure depending on the number of cycles. (PDF)

■ AUTHOR INFORMATION

Corresponding Author

*Maria Cazacu. E-mail: mcazacu@icmpp.ro.

ORCID

Codrin Tugui: 0000-0003-3680-3174

Maria Cazacu: 0000-0003-4952-5548

Notes

The authors declare no competing financial interest.

■ ACKNOWLEDGMENTS

This work was supported by a grant of the Romanian National Authority for Scientific Research and Innovation, CNCS/CCCDI-UEFISCDI, project number PN-III-P2-2.1-PED-2016-0188, within PNCDI III (Grant 68PED/2017) and by the project PolyWEC (www.polywec.org, prj. ref 309139), an FET-Energy project that was partially funded by the seventh Framework Programme of European Community.

■ REFERENCES

- (1) Pelrine, R.; Kornbluh, R.; Eckerle, J.; Jeuck, P.; Oh, S.; Pei, Q.; Stanford, S. Dielectric elastomers: generator mode fundamentals and applications. *Proc. SPIE* **2001**, 148–156.
- (2) Veretchy, R.; Fontana, M.; Rosati Papini, G. P.; Forehand, D. In-tank tests of a dielectric elastomer generator for wave energy harvesting. *Proc. SPIE* **2014**, 9056, 90561G.
- (3) Ahnert, K.; Abel, M.; Kollosche, M.; Jørgensen, P. J.; Kofod, G. Soft capacitors for wave energy harvesting. *J. Mater. Chem.* **2011**, 21 (38), 14492–14497.
- (4) Chiba, S.; Waki, M.; Wada, T.; Hirakawa, Y.; Masuda, K.; Ikoma, T. Consistent ocean wave energy harvesting using electroactive polymer (dielectric elastomer) artificial muscle generators. *Appl. Energy* **2013**, 104, 497–502.
- (5) Brochu, P.; Stoyanov, H.; Chang, R.; Niu, X.; Hu, W.; Pei, Q. Capacitive Energy Harvesting Using Highly Stretchable Silicone-Carbon Nanotube Composite Electrodes. *Adv. Energy Mater.* **2014**, 4 (3), 1300659.
- (6) Jean-Mistral, C.; Basrou, S.; Chaillout, J.-J. Dielectric polymer: scavenging energy from human motion. *Proc. SPIE* **2008**, 6927, 692716.
- (7) Chiba, S.; Waki, M.; Masuda, K.; Ikoma, T.; Osawa, H.; Suwa, Y. Innovative Power Generation System for Harvesting Wave Energy. *Innovative Power Generation System for Harvesting Wave Energy* **2012**, 1001–1006.
- (8) Madsen, F. B.; Daugaard, A. E.; Hvilsted, S.; Skov, A. L. The Current State of Silicone-Based Dielectric Elastomer Transducers. *Macromol. Rapid Commun.* **2016**, 37, 378–413.
- (9) Pelrine, R.; Kornbluh, R.; Kofod, G. High-strain actuator materials based on dielectric elastomers. *Adv. Mater.* **2000**, 12 (16), 1223–1225.
- (10) Stoyanov, H.; Brochu, P.; Niu, X.; Della Gaspera, E.; Pei, Q. Dielectric elastomer transducers with enhanced force output and work density. *Appl. Phys. Lett.* **2012**, 100 (26), 3–6.
- (11) Li, Y.; Samad, Y. A.; Taha, T.; Cai, G.; Fu, S. Y.; Liao, K. Highly Flexible Strain Sensor from Tissue Paper for Wearable Electronics. *ACS Sustainable Chem. Eng.* **2016**, 4 (8), 4288–4295.
- (12) Pelrine, R. E.; Kornbluh, R. D.; Joseph, J. P. Electrostriction of polymer dielectrics with compliant electrodes as a means of actuation. *Sens. Actuators, A* **1998**, 64 (1), 77–85.
- (13) Pelrine, R.; Kornbluh, R.; Eckerle, J.; Jeuck, P.; Oh, S.; Pei, Q.; Stanford, S. Dielectric Elastomers: Generator Mode Fundamentals and Applications. *Proc. SPIE* **2001**, 4329, 148–156.
- (14) Stiubianu, G.; Soroceanu, A.; Varganici, C. D.; Tugui, C.; Cazacu, M. Dielectric elastomers based on silicones filled with transitional metal complexes. *Composites, Part B* **2016**, 93, 236–243.
- (15) Quinsa, J. E. Q.; Alexandru, M.; Nüesch, F. A.; Hofmann, H.; Borgschulte, A.; Opris, D. M. Highly stretchable dielectric elastomer composites containing high volume fractions of silver nanoparticles. *J. Mater. Chem. A* **2015**, 3 (28), 14675–14685.
- (16) Iacob, M.; Stiubianu, G.; Tugui, C.; Ursu, L.; Ignat, M.; Turta, C.; Cazacu, M. Goethite nanorods as a cheap and effective filler for siloxane nanocomposite elastomers. *RSC Adv.* **2015**, 5 (56), 45439–45445.
- (17) Madsen, F. B.; Yu, L.; Skov, A. L. Self-Healing, High-Permittivity Silicone Dielectric Elastomer. *ACS Macro Lett.* **2016**, 5 (11), 1196–1200.
- (18) Madsen, F. B.; Dimitrov, I.; Daugaard, A. E.; Hvilsted, S.; Skov, A. L. Novel cross-linkers for PDMS networks for controlled and well distributed grafting of functionalities by click chemistry. *Polym. Chem.* **2013**, 4, 1700–1707.

- (19) Düinki, S. J.; Ko, Y. S.; Nüesch, F. a.; Opris, D. M. Self-Repairable, High Permittivity Dielectric Elastomers with Large Actuation Strains at Low Electric Fields. *Adv. Funct. Mater.* **2015**, *25* (16), 2467–2475.
- (20) Tugui, C.; Vlad, S.; Iacob, M.; Varganici, C. D.; Pricop, L.; Cazacu, M. Interpenetrating poly(urethane-urea)–polydimethylsiloxane networks designed as active elements in electromechanical transducers. *Polym. Chem.* **2016**, *7* (15), 2709–2719.
- (21) Brochu, P.; Stoyanov, H.; Niu, X.; Pei, Q. All-silicone prestrain-locked interpenetrating polymer network elastomers: free-standing silicone artificial muscles with improved performance and robustness. *Smart Mater. Struct.* **2013**, *22* (5), 055022.
- (22) Tugui, C.; Bele, A.; Tiron, V.; Hamciuc, E.; Varganici, C. D.; Cazacu, M. Dielectric elastomers with dual piezo-electrostatic response optimized through chemical design for electromechanical transducers. *J. Mater. Chem. C* **2017**, *5*, 824–834.
- (23) Tugui, C.; Cazacu, M.; Sacarescu, L.; Bele, A.; Stiubianu, G.; Ursu, C.; Racles, C. Full silicone interpenetrating bi-networks with different organic groups attached to the silicon atoms. *Polymer* **2015**, *77*, 312–322.
- (24) Tugui, C.; Stiubianu, G.; Iacob, M.; Ursu, C.; Bele, A.; Vlad, S.; Cazacu, M. Bimodal silicone interpenetrating networks sequentially built as electroactive dielectric elastomers. *J. Mater. Chem. C* **2015**, *3* (34), 8963–8969.
- (25) Rosset, S.; Shea, H. R. Flexible and stretchable electrodes for dielectric elastomer actuators. *Appl. Phys. A: Mater. Sci. Process.* **2013**, *110* (2), 281–307.
- (26) Böse, H.; Uhl, D. Dielectric elastomers with novel highly-conducting electrodes. *Proc. SPIE* **2013**, 8687, 86872O.
- (27) Cai, L.; Song, L.; Luan, P.; Zhang, Q.; Zhang, N.; Gao, Q.; Zhao, D.; Zhang, X.; Tu, M.; Yang, F.; et al. Super-stretchable, Transparent Carbon Nanotube-Based Capacitive Strain Sensors for Human Motion Detection. *Sci. Rep.* **2013**, *3*, 3048.
- (28) Liang, J.; Xu, Y.; Huang, Y.; Zhang, L.; Wang, Y.; Ma, Y.; Li, F.; Guo, T.; Chen, Y. Infrared-Triggered Actuators from Graphene-Based Nanocomposites. *J. Phys. Chem. C* **2009**, *113*, 9921–9927.
- (29) Zhu, J.; Wei, S.; Ryu, J.; Guo, Z. Strain-Sensing Elastomer/Carbon Nanofiber “Metacomposites”. *J. Phys. Chem. C* **2011**, *115*, 13215–13222.
- (30) Stoyanov, H.; Kolloosche, M.; Risse, S.; Waché, R.; Kofod, G. Soft conductive elastomer materials for stretchable electronics and voltage controlled artificial muscles. *Adv. Mater.* **2013**, *25* (4), 578–583.
- (31) Urdaneta, M. G.; Delille, R.; Smela, E. Stretchable Electrodes with High Conductivity and Photo-Patternability. *Adv. Mater.* **2007**, *19* (18), 2629–2633.
- (32) Rogers, J. A.; Someya, T.; Huang, Y. Materials and Mechanics for Stretchable Electronics. *Science (Washington, DC, U. S.)* **2010**, *327* (5973), 1603–1607.
- (33) Cheng, T.; Zhang, Y.; Zhang, J.; Lai, W.; Huang, W. High-performance free-standing PEDOT:PSS electrodes for flexible and transparent all-solid-state supercapacitors. *J. Mater. Chem. A* **2016**, *4*, 10493–10499.
- (34) Cheng, T.; Zhang, Y.-Z.; Yi, J.-P.; Yang, L.; Zhang, J.-D.; Lai, W.-Y.; Huang, W. Inkjet-printed flexible, transparent and aesthetic energy storage devices based on PEDOT:PSS/Ag grid electrodes. *J. Mater. Chem. A* **2016**, *4*, 13754–13763.
- (35) Han, S.; Hong, S.; Ham, J.; Yeo, J.; Lee, J.; Kang, B.; Lee, P.; Kwon, J.; Lee, S. S.; Yang, M.-Y.; Ko, S. H. Fast Plasmonic Laser Nanowelding for a Cu-Nanowire Percolation Network for Flexible Transparent Conductors and Stretchable Electronics. *Adv. Mater.* **2014**, *26* (33), 5808–5814.
- (36) Han, S.; Hong, S.; Yeo, J.; Kim, D.; Kang, B.; Yang, M.-Y.; Ko, S. H. Nanorecycling: Monolithic Integration of Copper and Copper Oxide Nanowire Network Electrode through Selective Reversible Photo-thermochemical Reduction. *Adv. Mater.* **2015**, *27*, 6397–6403.
- (37) Moon, H.; Lee, H.; Kwon, J.; Suh, Y. D.; Kim, D. K.; Ha, I.; Yeo, J.; Hong, S.; Ko, S. H. Ag/Au/Polypyrrole Core-shell Nanowire Network for Transparent, Stretchable and Flexible Supercapacitor in Wearable Energy Devices. *Sci. Rep.* **2017**, *7*, 41981–10.
- (38) Yao, S.; Zhu, Y. Nanomaterial-enabled stretchable conductors: Strategies, materials and devices. *Adv. Mater.* **2015**, *27* (9), 1480–1511.
- (39) Lee, P.; Lee, J.; Lee, H.; Yeo, J.; Hong, S.; Nam, K. H.; Lee, D.; Lee, S. S.; Ko, S. H. Highly Stretchable and Highly Conductive Metal Electrode by Very Long Metal Nanowire Percolation Network. *Adv. Mater.* **2012**, *24*, 3326–3332.
- (40) Lee, P.; Ham, J.; Lee, J.; Hong, S.; Han, S.; Suh, Y. D.; Lee, S. E.; Yeo, J.; Lee, S. S.; Lee, D.; Ko, S. H. Highly Stretchable or Transparent Conductor Fabrication by a Hierarchical Multiscale Hybrid Nanocomposite. *Adv. Funct. Mater.* **2014**, *24* (36), 5671–5678.
- (41) Kim, K. K.; Hong, S.; Cho, H. M.; Lee, J.; Suh, Y. D.; Ham, J.; Ko, S. H. Highly Sensitive and Stretchable Multidimensional Strain Sensor with Prestrained Anisotropic Metal Nanowire Percolation Networks. *Nano Lett.* **2015**, *15* (8), 5240–5247.
- (42) Cheng, T.; Zhang, Y.; Lai, W. Y.; Huang, W. Stretchable thin-film electrodes for flexible electronics with high deformability and stretchability. *Adv. Mater.* **2015**, *27* (22), 3349–3376.
- (43) Hong, S.; Lee, H.; Lee, J.; Kwon, J.; Han, S.; Suh, Y. D.; Cho, H.; Shin, J.; Yeo, J.; Ko, S. H. Highly Stretchable and Transparent Metal Nanowire Heater for Wearable Electronics Applications. *Adv. Mater.* **2015**, *27* (32), 4744–4751.
- (44) Jeong, C. K.; Lee, J.; Han, S.; Ryu, J.; Hwang, G.; Park, D. Y.; Park, J. H.; Lee, S. S.; Byun, M.; Ko, S. H.; et al. A Hyper-Stretchable Elastic-Composite Energy Harvester. *Adv. Mater.* **2015**, *27* (18), 2866–2875.
- (45) Lee, H.; Hong, S.; Lee, J.; Suh, Y. D.; Kwon, J.; Moon, H.; Kim, H.; Yeo, J.; Ko, S. H. Highly Stretchable and Transparent Supercapacitor by Ag – Au Core – Shell Nanowire Network with High Electrochemical Stability. *ACS Appl. Mater. Interfaces* **2016**, *8* (24), 15449.
- (46) Cheng, T.; Zhang, Y.; Lai, W.; Chen, Y.; Zeng, W.; Huang, W. High-performance stretchable transparent electrodes based on silver nanowires synthesized via an eco-friendly halogen-free method. *J. Mater. Chem. C* **2014**, *2*, 10369–10376.
- (47) Ashfold, M. N. R.; Claeysens, F.; Fuge, G. M.; Henley, S. J. Pulsed laser ablation and deposition of thin films. *Chem. Soc. Rev.* **2004**, *33* (1), 23–31.
- (48) Rosset, S.; Araromi, O. A.; Schlatter, S.; Shea, H. R. Fabrication Process of Silicone-based Dielectric Elastomer Actuators. *J. Visualized Exp.* **2016**, 53423 (108), 53423.
- (49) Moretti, G.; Fontana, M.; Vertechy, R. Model-based design and optimization of a dielectric elastomer power take-off for oscillating wave surge energy converters. *Meccanica* **2015**, *50* (11), 2797–2813.
- (50) Moretti, G.; Fontana, M.; Vertechy, R. Parallelogram-shaped dielectric elastomer generators: Analytical model and experimental validation. *J. Intell. Mater. Syst. Struct.* **2015**, *26* (6), 740–751.
- (51) Vertechy, R.; Papini Rosati, G. P.; Fontana, M. Reduced Model and Application of Inflating Circular Diaphragm Dielectric Elastomer Generators for Wave Energy Harvesting. *J. Vib. Acoust.* **2015**, *137* (1), 011016.
- (52) Maas, J.; Graf, C. Dielectric elastomers for hydro power harvesting. *Smart Mater. Struct.* **2012**, *21*, 064006.
- (53) Yin, G.; Yang, Y.; Song, F.; Renard, C.; Dang, Z.; Shi, C.; Wang, D. Dielectric Elastomer Generator with Improved Energy Density and Conversion Efficiency Based on Polyurethane Composites. *ACS Appl. Mater. Interfaces* **2017**, *9*, 5237–5243.
- (54) Cazacu, M.; Marcu, M. Silicone Rubbers. IX. Contributions to Polydimethylsiloxane- α,ω -Diols Synthesis by Heterogeneous Catalysis. *J. Macromol. Sci., Part A: Pure Appl. Chem.* **1995**, *32* (sup7), 1019–1029.
- (55) Li, J. C.; Wang, Y.; Ba, D. C. Characterization of Semiconductor Surface Conductivity by Using Microscopic Four-Point Probe Technique. *Phys. Procedia* **2012**, *32*, 347–355.